ENOC-2008, Saint Petersburg, Russia, June, 30–July, 4 2008

TWO VAN DER POL-DUFFING OSCILLATORS WITH HUYGENS COUPLING

V.N. Belykh, E.V. Pankratova
Mathematics Department
Volga State Academy
Nizhny Novgorod, 603600, Russia.
Belykh@unn.ac.ru, Pankratova@aqua.sci-nnov.ru

A.Yu. Pogromsky, H. Nijmeijer
Department of Mechanical Engineering
Eindhoven University of Technology
PO Box 513 5600 MB Eindhoven, The Netherlands.
A.Pogromsky@tue.nl, H.Nijmeijer@tue.nl

Abstract
We consider a system of two Van der Pol-Duffing oscillators with Huygens (speeding up) coupling. This system serves as appropriate model for Huygens synchronization of two mechanical clocks hanging from a common support. We examine the main regimes of complete and phase synchronization, and study the dependence of their onset on the initial conditions. In particular, we reveal co-existence of two chaotic phase synchronized modes and study the structure of their complicated riddled basins.

Key words
Synchronization, Van der Pol-Duffing oscillator, coupled systems, chaotic oscillations

1 Introduction

Synchronization phenomena have been the subject of discussion in various research areas since the 17th century, when the synchronization of two pendulum clocks attached to a common support beam was first discovered by Cristian Huygens [Huygens, 1673]. Later, the findings of Huygens were reproduced by means of similar setups in both experimental and theoretical works [Blekhman, 1998; Bennett *et al.*, 2002; Pantaleone, 2002].

In a recent paper [Oud, Nijmeijer and Pogromsky, 2006] synchronization experiments with a setup consisting of driven pendula were performed. Particular attention was paid to different synchronization regimes that can be observed in this situation: anti-phase and in-phase synchronization which are two typical synchronization regimes observed in the experimental setup. Historically, anti-phase synchrony was originally observed by Huygens while in-phase synchronization in a Huygens-type setup was observed and explained in [Blekhman, 1998] by means of a model of coupled van der Pol equations.

Here, we examine a model of Huygens original system that consists of two oscillators driven by the Van der Pol-Duffing control input, providing the escape mechanism. Both oscillators are connected to a movable platform via a spring. Due to this coupling the oscillators influence each other and can synchronize. This paper investigates the onset of synchronous regimes in the two-oscillator setup and their dependence on the initial conditions and parameters of the coupled system.

2 Problem statement

The mathematical mechanism behind the remarkable Huygens' observation of synchronized mechanical clocks hanging from a common support was recently described in [Pogromsky, Belykh and Nijmeijer, 2003]. The model used is the following. A beam of mass M can move in the horizontal direction with viscous friction defined by damping coefficient d. One side of the beam is attached to the wall via a spring with elasticity k. The beam supports two identical pendula of length l and mass m. The torque applied to each pendulum is to sustain the clock active mode of pendula. It can also be viewed as a control input, introducing the escape mechanism to the system. The system equations can be written in the form of Euler-Lagrange equations:

$$\begin{aligned} &ml^2\ddot{\phi}_1 + mgl\sin\phi_1 + f_1 = -ml\ddot{y}\cos\phi_1 \\ &ml^2\ddot{\phi}_2 + mgl\sin\phi_2 + f_2 = -ml\ddot{y}\cos\phi_2 \\ &(M+2m)\ddot{y} + d\dot{y} + ky = \\ &\qquad -ml\sum_{i=1}^{2}(\ddot{\phi}_i\cos\phi_i - \dot{\phi}_i^2\sin\phi_i), \end{aligned} \tag{1}$$

where $\phi_i \in S^1$ is the angular displacement of the i-th pendulum about its pivot point, y is the linear displacement of the beam, and f_1, f_2 are the control inputs defining the escape mechanism.

The Hamiltonian for each unperturbed pendulum

($f_i \equiv 0, y \equiv 0$) has the form:

$$H(\phi_i, \dot{\phi}_i) = \frac{ml^2\dot{\phi}_i^2}{2} + mgl(1 - \cos\phi_i), \quad (2)$$

Here, in contrast to [Pogromsky, Belykh and Nijmeijer, 2003], we use the only angle dependent control input

$$f_i = \gamma\dot{\phi}_i[H(\phi, 0) - H_*], \quad (3)$$

and get a simple model of the pendulum

$$ml^2\ddot{\phi} + \gamma\dot{\phi}[H(\phi, 0) - H_*] + mgl\sin\phi = 0. \quad (4)$$

Defined on the cylinder $(\phi, \dot{\phi})$, system (4) has an unstable equilibrium point $(\phi = \dot{\phi} = 0)$, enveloped by a stable limit cycle which turns into a heteroclinic contour of the saddle point $(\phi = \pi, \dot{\phi} = 0)$ when parameter $H_* > 0$ increases [Belyustina and Belykh, 1973]. Since the clock angular displacement is fairly small (there is no rotation), the parameter H_* must be small, and one can pass to the linear displacement of pendula $x_i = l\phi_i$ using shortened expansions in (1), (4).

$$\begin{array}{ll} \cos\phi = 1 - \frac{x^2}{2l^2} + \ldots, & \sin\phi = \frac{x}{l} - \frac{x^3}{6l^3} + \ldots, \\ H(\phi, 0) = mg\frac{x^2}{2l} + \ldots, & \ddot{y}\cos\phi = \ddot{y} + \ldots, \\ \ddot{\phi}\cos\phi = \ddot{\phi} + \ldots, & \dot{\phi}^2\sin\phi = 0. \end{array} \quad (5)$$

Obviously, this expansion is valid for a large enough values of l. Hence, the system (1) attains the form:

$$\begin{array}{l} \ddot{x}_1 + \lambda(x_1^2 - 1)\dot{x}_1 + \omega^2 x_1 - \alpha x_1^3 = -\ddot{y} \\ \ddot{x}_2 + \lambda(x_2^2 - 1)\dot{x}_2 + \omega^2 x_2 - \alpha x_2^3 = -\ddot{y} \\ (M + 2m)\ddot{y} + d\dot{y} + ky = -m(\ddot{x}_1 + \ddot{x}_2), \end{array} \quad (6)$$

where $\lambda = \frac{\gamma g}{2l^3}$, $\omega = \sqrt{g/l}$, $\alpha = \frac{g}{6l^3}$.

The system (6) can be rewritten in the following form

$$\begin{array}{l} \ddot{x}_1 + \omega^2 x_1 + F(x_1, \dot{x}_1) = -\mu\ddot{y}, \\ \ddot{x}_2 + \omega^2 x_2 + F(x_2, \dot{x}_2) = -\mu\ddot{y}, \\ \ddot{y} + h\dot{y} + \Omega^2 y = m[\omega^2(x_1 + x_2) + \sum_{i=1}^{2} F(x_i, \dot{x}_i)], \\ \dot{x}_1 = u_1, \dot{x}_2 = u_2, \dot{y} = z. \end{array} \quad (7)$$

Here, $F(x_i, \dot{x}_i) = \lambda(x_i^2 - 1)\dot{x}_i - \alpha x_i^3, i = 1, 2$, and new notations for the coupling parameter $\mu = 1/M$, frequency of the platform $\Omega = \sqrt{k/M}$ and damping factor $h = d/M$ were introduced. Note that new y stands for μy. Thus, the Huygens problem is now transformed to the synchronization problem of two van der Pol-Duffing oscillators with the special coupling which we call "Huygens coupling". Note that for $\alpha = 0$ and $\lambda \ll 1$ such an approach was used in [Blekhman, 1998].

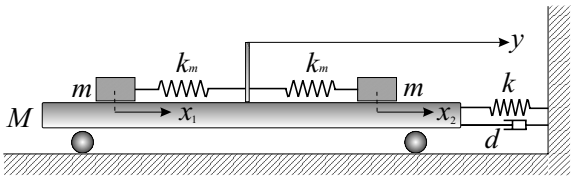

Figure 1. Schematic drawing of the system, which consists of two oscillators with masses m coupled via the platform with mass M.

For the linear displacement x_i the equations (7) model the Nijmeijer setup described in [Oud, Nijmeijer and Pogromsky, 2006] and depicted in Fig.1. The platform of the mass M is attached to the wall via a spring with linear stiffness k and a damper with viscous friction coefficient d. Due to its possible horizontal displacement the platform couples the dynamics of two oscillators with masses m. Both oscillators are connected to the platform via a spring with linear stiffness k_m and driven by force $F(x_i, \dot{x}_i) = \lambda(x_i^2 - 1)\dot{x}_i - \alpha x_i^3, i = 1, 2$. In the setup shown in Fig.1 the frequency of each m-mass oscillator is $\omega = \sqrt{k_m/m}$. In Eq.(7) $x_{1,2}$ and y are the vibrations of oscillators and platform, respectively; $u_{1,2}$ and z are the velocities of motion of the oscillators and platform, respectively.

The conservative system (6), with $\lambda = d = 0$ has the integral

$$V = \sum_{i=1}^{2} m\left(\frac{\omega^2 x_i^2}{2} - \frac{\alpha x_i^4}{4} + \frac{\dot{x}_i^2}{2} + \dot{x}_i\dot{y}\right) + (M + 2m)\frac{\dot{y}^2}{2} + k\frac{y^2}{2} = const \quad (8)$$

which serves as the Lyapunov-like function for the system with the damped platform, $\lambda = 0, d > 0$:

$$\dot{V} = -d\dot{y}^2 \leq 0.$$

The latter implies that conservative oscillators together with the platform for $d > 0$ return to the stable equilibrium point at the origin, provided that initial perturbations are bounded.

Our goal is to study synchronization phenomena when the escape mechanism is switched on, i.e. $\lambda > 0$. From the equations of the model it follows that the system (6), as well as the system (7), has two invariant manifolds: the 4-d in-phase manifold $M_s := \{(x_1, u_1) = (x_2, u_2)\}$ and the 2-d anti-phase manifold $M_a := \{(x_1, u_1) = (-x_2, -u_2), y = z = 0\}$. The system (7) possess two symmetries defining the existence of the two manifolds: the invariance under the maps

$$\begin{array}{l} (x_1, x_2) \to (x_2, x_1) \\ (u_1, u_2) \to (u_2, u_1) \end{array} \quad (9)$$

and

$$(x_1, x_2, y) \to (-x_1, -x_2, -y)$$
$$(u_1, u_2, z) \to (-u_1, -u_2, -z) \qquad (10)$$

The map (9) defines the mirror symmetry with respect to M_s, while the transformation (10) gives the central symmetry with respect to M_a.

From existence of manifolds, and from symmetries (9), (10) it follows that the system (7) may have a synchronous attractor A_s lying in M_s, the an anti-phase attractor A_a contained in M_a. Besides A_s and A_a, there may exist either a symmetrical attractor A_{sym} lying outside of $(M_s \cup M_a)$ or two asymmetrical attractors A^+_{asym}, A^-_{asym} being symmetrical to each other via (9), (10). Obviously, the attractors may coexist in the phase space of the system (7). Our main purpose is to study these attractors and the structure of their basins.

3 Synchronization of oscillators driven by Van der Pol control input

We start with the case where both oscillators are driven by the force $F(x_i, \dot{x}_i) = \lambda(x_i^2 - 1)\dot{x}_i, i = 1, 2$. Thus, for $\mu = 0$, the behavior of each oscillator is defined by a solution of the differential equation, known as the van der Pol equation. The parameter λ defines the form of the limit cycle: for small λ the motion of oscillator is quasi-harmonic, for large λ the relaxation oscillations are observed. We consider the case, where the frequencies of the oscillators and platform are equal. The similar situation was considered in [Oud, Nijmeijer and Pogromsky, 2006], where the experiments with the frequency of the platform which is close to or above the frequency of the metronomes have been performed. We assume that $\omega = \Omega = 1$. Experimentally, to prevent the situation when oscillations of the platform become too large and the metronomes will hit the frame of the setup, the authors of [Oud, Nijmeijer and Pogromsky, 2006] used (increased) magnetic damping. In our theoretical study we assume that $h = 0.5$.

For $\mu \neq 0$ the platform couples both oscillators. Since the coupling parameter μ is inversely proportional to the mass of the platform M, a decrease in M leads to an increase in μ. In his original experiment, Huygens used a massive beam to couple the clocks and found that phase locking in anti-phase regime was robust [Huygens, 1673]. However, it was shown later, that the synchronization of two metronomes resting on a light wooden board [Pantaleone, 2002] generally appeared in the form of an in-phase motion. Both the situations can easily be modeled and confirmed in our setting as limit cases for small and large μ, respectively. In the present work, we examine the intermediate case and consider the two following values for the coupling parameter: $\mu = 0.5$ and $\mu = 1$. Let us first focus on the case where $\mu = 0.5$. For various λ the limit sets for the trajectory starting from the phase

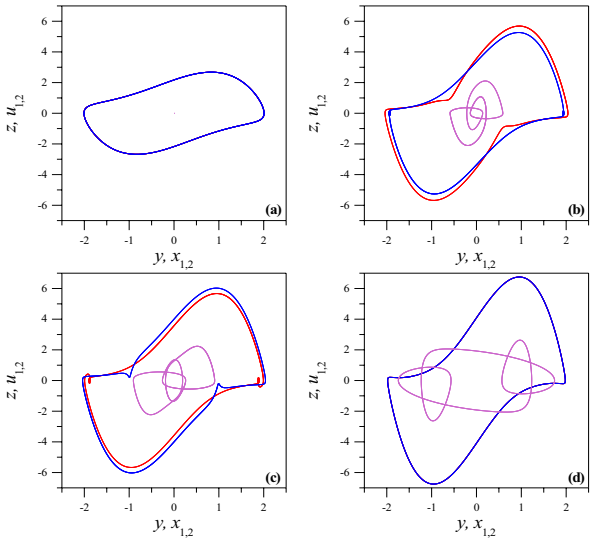

Figure 2. Projections of the phase portrait onto the planes (x_1, u_1) - red curves, (x_2, u_2) - blue curves, and (y, z) - violet curves for various values of parameter λ. For all the curves initial conditions are the same $(x_1^0, x_2^0) = (0.4, -0.1)$. (a) $\lambda = 1$; (b) $\lambda = 2.64$; (c) $\lambda = 2.8$; (d) $\lambda = 3$. Parameters are: $\alpha = 0, \Omega = \omega = 1, \mu = 0.5, h = 0.5, m = 0.47$.

point $(x_1^0, x_2^0) = (0.4, -0.1)$ are shown in Fig.2 in projections onto the (displacement, velocity)-planes. The initial values for other variables are assumed to be zero.

Obviously, that for identical oscillators in anti-phase regime the total force would be the zero and due to the damper, oscillations of the platform die out, Fig2(a). When the dynamics of oscillators is on attractors A^+_{asym} or A^-_{asym}, Fig2(b), (c) as well as for the completely synchronous movement of both oscillators observed in in-phase regime, Fig2(d), oscillations of the platform appear.

The basins of attractors corresponding to these oscillatory regimes are shown in Fig.3 in projection onto the (x_1, x_2)-plane. In order to obtain these diagrams, we have changed initial displacements of both oscillators within the range $X := \{(x_1^0, x_2^0) | x_1^0 \in [-3, 3], x_2^0 \in [-3, 3]\}$. Initial values for other variables were assumed to be equal to zero.

For small λ both oscillators only oscillate in either anti-phase or in-phase modes, Fig.3(a), (b). In the figures the anti-phase synchronization ($A_a \subset M_a := \{(x_1, u_1) = (-x_2, -u_2), y = z = 0\}$) is established for initial oscillators' displacements falling into the yellow ranges. Basins of attraction corresponding to the in-phase synchronization ($A_s \subset M_s := \{(x_1, u_1) = (x_2, u_2)\}$) are shown in green. For $\lambda \gtrsim 2.63$ for some initial conditions the dynamics of oscillators can also obey various regular symmetrical to each other attractors A^+_{asym} or A^-_{asym}. The basins of these attracting sets are shown as red and blue domains in Fig.3(c), (d). For large enough λ, attractor A_a belonging to the manifold M_a and corresponding to oscillations in anti-phase regime, loses its stability. In this case three stable periodic orbits co-exist in phase space of the system (7):

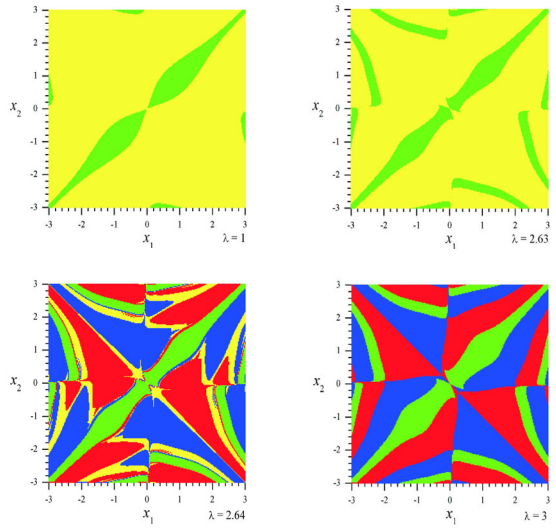

Figure 3. Basins of attraction in projections onto the (x_1, x_2) plane for various values of parameter λ. The domains for anti-phase synchronization ($(x_1, u_1) = (-x_2, -u_2)$) are shown in yellow, whereas the green domains correspond to in-phase synchronization ($(x_1, u_1) = (x_2, u_2)$). The basins of attractors A^+_{asym} and A^-_{asym} are shown in red and blue, respectively. The parameters of the system are: $\alpha = 0, \Omega = \omega = 1, \mu = 0.5, h = 0.5, m = 0.47$.

A^+_{asym}, A^-_{asym} and A_s, belonging to the diagonal M_s. For $\lambda = 3$ the basins of these attractors in projections onto the (x_1, x_2) plane are shown in Fig.3(d). Note that the structures shown in Fig.3 were obtained for zero values of initial oscillators' velocities. Otherwise, if $u_1^0 \neq u_0^2$, the symmetry observed in Fig.3 is broken.

When $\mu = 1$ for small and large values of λ the structures of attractors similar to Fig.3(a), (d) are observed. However, the transition from the double-state $\{A_s$ and $A_a\}$ to the triple-state $\{A_s, A^+_{asym}$ and $A^-_{asym}\}$ regime occurs differently. To illustrate this we consider a one-parameter bifurcation diagram for increasing λ, obtained for the fixed initial displacements of oscillators: $(x_1^0, x_2^0) = (-0.7, -2.0)$, Fig.4. In this figure, x_2 is the value of displacement of the second oscillator being the point of intersection of the trajectory with the hyperplane $\mathcal{P} : \{x_1 = 0.1\}$. As seen from Fig.4, the

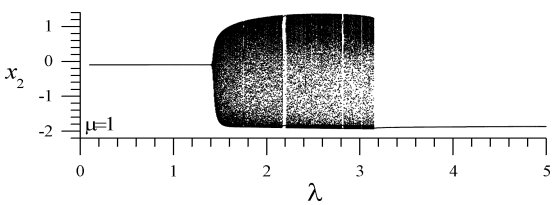

Figure 4. Rearrangement of attracting sets on the one-parametric bifurcation diagram for $\mu = 1$. The initial displacements of oscillators are $(x_1^0, x_2^0) = (-0.7, -2.0)$.

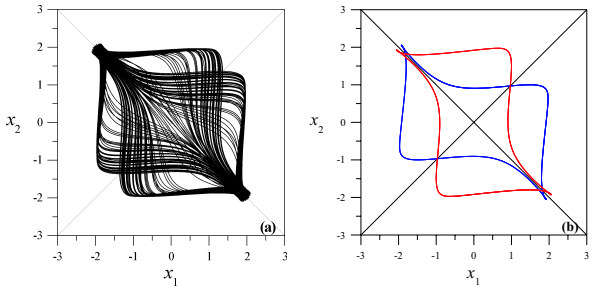

Figure 5. Projections of phase portrait onto the (x_1, x_2) plane for $\mu = 1$ and (a) $\lambda = 3$, (b) $\lambda = 3.2$.

transition from double-state to triple-state behavior for $\mu = 1$ via chaotic regime occurs. Experimentally, the existence of such type of oscillations was also observed in [Oud, Nijmeijer and Pogromsky, 2006]. In Fig.5(a) the projection of a chaotic attractor onto the (x_1, x_2) plane for $\lambda = 3$ is presented. When $\lambda = 3.2$, as for $\mu = 0.5$, two regular, symmetrical to each other attractors A^+_{asym} or A^-_{asym} are observed, Fig.5(b).

In order to show existence of phase synchronization for oscillators, we calculate the phases of their oscillations. In our case, since the center of rotation can clearly be distinguished at $(x_i, u_i) = (0, 0), i = 1, 2$, Fig.2, the following definition of the phase can be used:

$$\theta_{1,2} = \arctan(u_{1,2}/x_{1,2}). \tag{11}$$

For various values of parameters we check whether the locking condition

$$\Delta\theta = |\theta_1 - \theta_2| < const < 2\pi \tag{12}$$

is satisfied. In Fig.6 the phase difference $\Delta\theta$ for regular ($\lambda = 3.2$) and chaotic ($\lambda = 3$) motions of oscillators is given. For both the cases $\Delta\theta$ is a bounded function. Accordingly, phase synchronization is observed

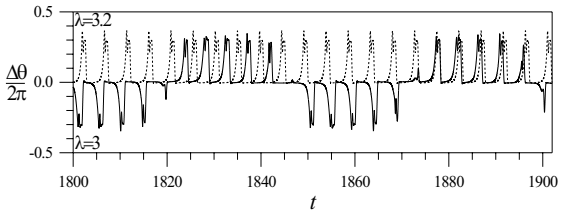

Figure 6. Phase difference $\Delta\theta$ for $\lambda = 3$ - solid line, and $\lambda = 3.2$ - dotted line, $\mu = 1$. Here, $\Delta\theta < \pi$.

for both regular and chaotic motions in the considered setup.

4 Synchronization of oscillators driven by Van der Pol-Duffing control input

In this section we assume that both oscillators are driven by the force $F(x_i, \dot{x}_i) = \lambda(x_i^2 - 1)\dot{x}_i - \alpha x_i^3, i =$

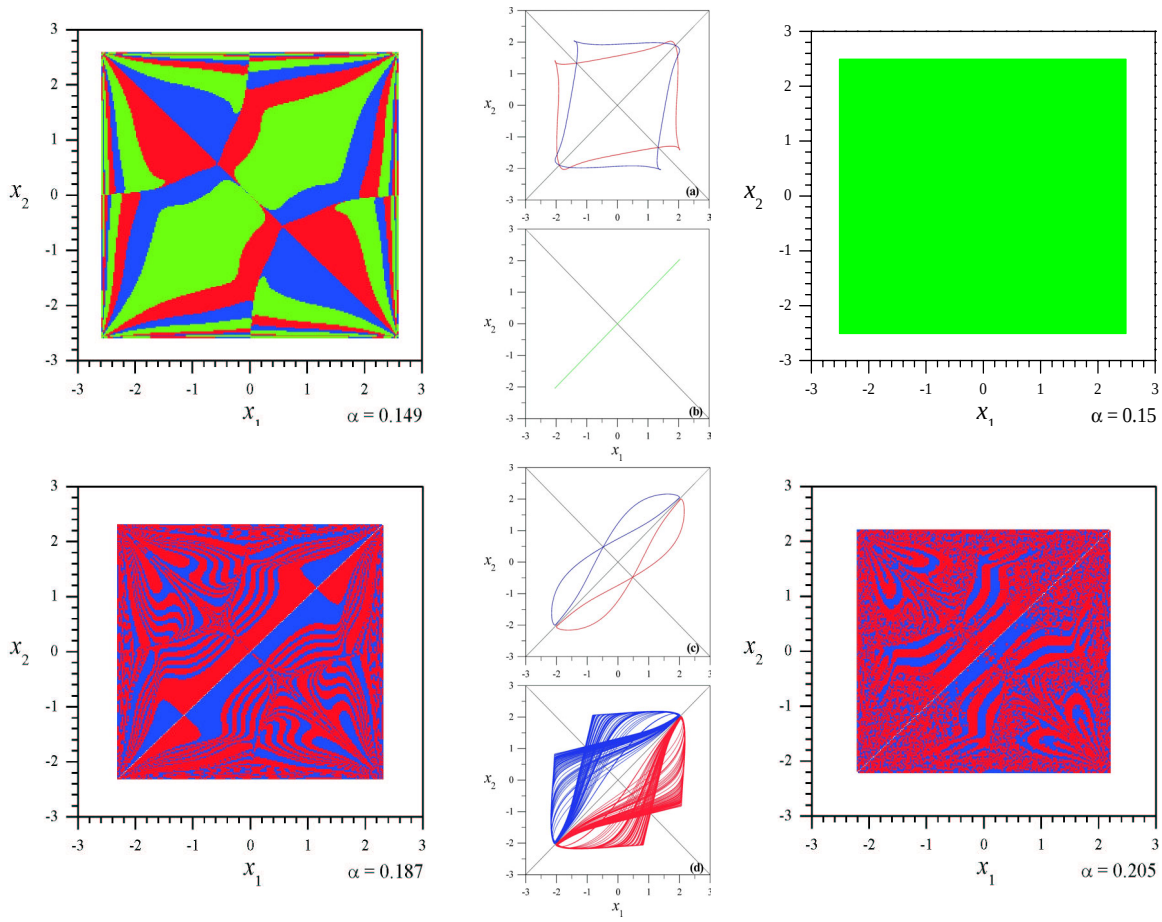

Figure 7. Basins of attraction in projections onto the (x_1, x_2) plane for various values of parameter α. The in-phase synchronization ($(x_1, u_1) = (x_2, u_2)$) is established for initial displacements of oscillators falling into the green ranges. The ranges shown in red and blue correspond to the case of phase synchronization when the dynamics of each oscillator is defined by various, symmetrical to each other attractors A^+_{asym} and A^-_{asym}. The parameters of the system (7) are: $\lambda = 2.5, \Omega = 0.3, \omega = 1, \mu = 1, h = 0.01, m = 0.47$.

$1, 2$, and focus on changes in the behavior of oscillators occurring with the increase of α. Depending on the parameters, the structure of the phase space for individual oscillator ($\mu = 0$) can be different [Belyustina and Belykh, 1973]. For small values of α the unstable trivial equilibrium point $x^* = 0$ is enveloped by a stable limit cycle. The influence of two saddle points $x^* = \pm\omega/\sqrt{\alpha}$ in this case can be neglected. With the increase of α both saddle points move to each other resulting in formation of a heteroclinic contour of saddle points for some value $\alpha = \alpha_h$. While α reaches α_h the limit cycle "grows into" this heteroclinic contour. For $\alpha > \alpha_h$ the limit cycle disappears.

For the system (7) there are nine equilibrium points. All of these states are of saddle type. The structure of basins for attractors in system (7) under Van der Pol-Duffing control input for various values of parameter α and fixed other parameters ($\lambda = 2.5, \Omega = 0.3, \omega = 1, \mu = 1, h = 0.01, m = 0.47$) is shown in Fig.7. Note that similar structures for parameters considered in the previous section, with increasing α can also be observed. For small α three various attracting sets co-exist in the system: $A_s \subset M_s$, and two symmetrical to each other attractors A^+_{asym} and A^-_{asym}, Fig.7(a). The increase of α leads to disappearance (at $\alpha = \alpha^* \approx 0.15$) of attractors A^+_{asym} and A^-_{asym}, Fig.7(b). For $\alpha = \alpha^*$ the manifolds of nontrivial equilibrium points divide the phase space of the system into two parts: the part of completely synchronous motion $S : \{(x_1, x_2)||x_1| < \omega/\sqrt{\alpha^*}, |x_2| < \omega/\sqrt{\alpha^*}\}$ (green range in Fig.7) and the part of unstable motion $U : \{(x_1, x_2)||x_1| > \omega/\sqrt{\alpha^*}, |x_2| > \omega/\sqrt{\alpha^*}\}$. This regime is preserved for $\alpha \in (0.15; 0.18)$. For $\alpha \approx 0.187$ the attractor A_s loses its asymptotic transverse stability via a *riddling bifurcation* [Lai *et al.*, 1996]. After the riddling bifurcation, the system has two new stable periodic solutions $\widetilde{A}^+_{asym}$ and $\widetilde{A}^-_{asym}$, Fig.7(c). For $\alpha = 0.205$ the complex (riddled) structure of basin for chaotic attractors is shown in Fig.7(d). The phase portrait of the system in projections onto the (x_1, u_1) and (y, z) planes for $\alpha = 0.205$ is shown in Fig.8(a), (b). The following increase of α leads to the appearance of a more complicated chaotic attractor, Fig.8(c), (d).

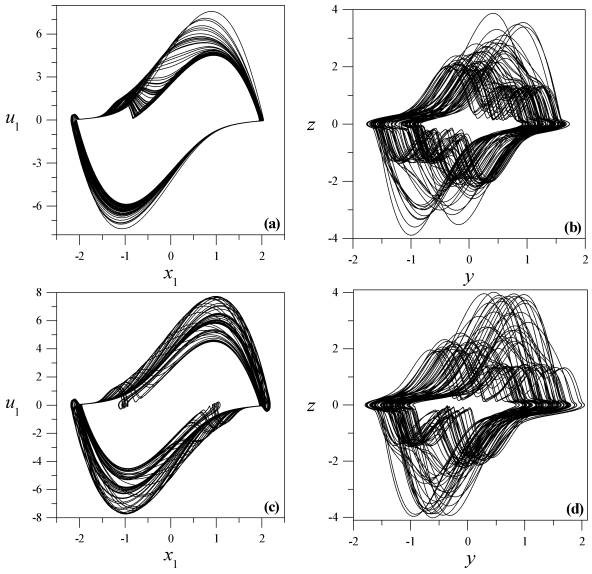

Figure 8. Projections of phase portrait onto the (x_1, u_1) and (y, z) planes for (a), (b) $\alpha = 0.205$ and (c), (d) $\alpha = 0.21$.

To illustrate rearrangement of attracting sets in the system (7) we consider a one-parameter bifurcation diagram for increasing α, Fig.9. In this figure, as before, x_2 is the value of displacement for the second oscillator being the point of intersection of the trajectory with the hyperplane $\mathcal{P} : \{x_1 = 0\}$. The initial conditions were taken close to the diagonal M_s, namely $(x_1^0, x_2^0) = (0.0, -0.1)$. Therefore, for $0 < \alpha < 0.187$ the behavior of both oscillators are completely synchronous: x_1 and x_2 intersect $\mathcal{P}$ at the same time. For $0.187 < \alpha < 0.202$, depending on the initial

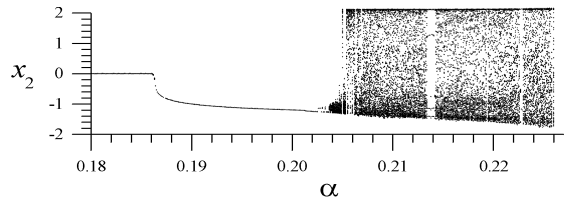

Figure 9. Transition to chaos in the one-parametric bifurcation diagram with the increase of α. The initial displacements of oscillators are $(x_1^0, x_2^0) = (0.0, -0.1)$.

conditions we observe two various values of displacement for the second oscillator (it is omitted in Fig.9 for brevity). In this interval of α two various but symmetrical to each other periodic motions $\widetilde{A}^+_{asym}$ and $\widetilde{A}^-_{asym}$ co-exist. The chaotic oscillations arise at $\alpha \approx 0.203$ and preserve in a wide range of α. However, despite this complexity of motion, both oscillators exhibit the phase synchronous behavior.

5 Conclusions

In the present work we have considered the system of two oscillators connected to a movable platform via a spring. The platform couples the dynamics of both oscillators causing their synchronous movement. In order to analyze possible regimes of their synchronous motion the numerical simulation has been performed for two types of control input: Van der Pol and Van der Pol-Duffing. It was shown that depending on the initial conditions and parameters of the system, three synchronous regimes are possible: complete ($(x_1, u_1) = (x_2, u_2)$), anti-phase ($(x_1, u_1) = (-x_2, -u_2)$) and phase synchronization. For the latter regime the amplitudes of two oscillators remain quite different, while the locking between the phases has been observed, i.e. $\Delta\theta = |\theta_1 - \theta_2| < const < 2\pi$. The existence of this regime for both regular and irregular motions in the setup has been revealed. Phase synchronization implies that despite both the complexity of motion and difference in oscillator displacements the clocks show the same time.

Acknowledgements

This work was supported in part by the Russian Foundation for Basic Research (grants No. 05-01-00509 and No. 07-02-01404) and the Dutch-Russian program Dynamics and Control of Hybrid Mechanical Systems (DyCoHyMS) (NWO-RFBR grant 047.017.018). E.V.P. also acknowledges the support of the Dynasty Foundation.

References

Belyustina, L.N. and Belykh, V.N. (1973) Qualitative analysis of dynamical system on cylinder. *Differents. Uravneniya*, **9**(3), pp. 403–415.

Bennett, M., Schatz, M., Rockwood, H. and Wiesenfeld, K. (2002) Huygenss clocks. *Proc. R. Soc. Lond. A*, **458**(2019), pp. 563-579.

Blekhman, I.I. (1998). *Synchronization in science and technology*. ASME. New York.

Huygens, C. (1673) *Horoloquim Oscilatorium*. Apud F. Muguet, Parisiis, France; English translation: *The pendulum clock*, 1986, Iowa State University Press, Ames.

Lai, Y.-C., Grebogi, C., Yorke, J.A. and Venkataramani, S.C. (1996) Riddling bifurcation in chaotic dynamical systems. *Phys. Rev. Lett.*, **77**, pp. 55-58.

Oud, W.T., Nijmeijer, H. and Pogromsky, A.Yu. (2006) A study of Huijgens synchronization. Experimental results, in *Group Coordinationi and Control*, K.Y. Pettersen, J.T. Gravdahl, H. Nijmeijer (eds), Springer, 2006.

Pantaleone, J. (2002) Synchronization of metronomes. *American Journal of Physics*, **70**(10), pp. 992-1000.

Pogromsky, A.Yu., Belykh, V.N. and Nijmeijer, H. (2003). Controlled synchronization of pendula. In *Proc. of the 42nd IEEE Conference on Decision and Control*. Maui, Hawaii USA, December . pp. 4381–4386.

Pogromsky, A.Yu., Belykh, V.N. and Nijmeijer, H. (2006). A study of controlled synchronization of Hui-

jgens pendula. In *Lecture Notes in Control and Information Sciences. Group Coordination and Cooperative Control.*, **336**, pp. 205–216. Springer Berlin. Heidelberg.

Van der Pol, B. (1922) Theory of the amplitude of free and forced triod vibration. *Radio Rev.*, **1**, pp. 701-710.